Temperature-Dependent Rate Coefficients for the Reactions of $Br(^2P_{3/2})$, $Cl(^2P_{3/2})$, and $O(^3P_J)$ with $BrONO_2$†

R. Soller,‡,|| J. M. Nicovich,§ and P. H. Wine*,‡,§

School of Earth and Atmospheric Sciences and School of Chemistry and Biochemistry, Georgia Institute of Technology, Atlanta, Georgia 30332

Received: May 26, 2000; In Final Form: August 10, 2000

A laser flash photolysis−resonance fluorescence technique has been employed to investigate the kinetics of reactions of the important stratospheric species bromine nitrate ($BrONO_2$) with ground-state atomic bromine (k_1), chlorine (k_2), and oxygen (k_3) as a function of temperature (224−352 K) and pressure (16−250 Torr of N_2). The rate coefficients for all three reactions are found to be independent of pressure and to increase with decreasing temperature. The following Arrhenius expressions adequately describe the observed temperature dependencies (units are 10^{-11} $cm^3 molecule^{-1} s^{-1}$): $k_1 = 1.78 \exp(365/T)$, $k_2 = 6.28 \exp(215/T)$, and $k_3 = 1.91 \exp(215/T)$. The accuracy of reported rate coefficients is estimated to be 15−25% depending on the magnitude of the rate coefficient and on the temperature. Reaction with atomic oxygen is an important stratospheric loss process for bromine nitrate at altitudes above ∼25 km; this reaction should be included in models of stratospheric chemistry if bromine partitioning is to be correctly simulated in the 25−35 km altitude regime.

Introduction

Bromine nitrate ($BrONO_2$) is a key stratospheric chemical species, serving both as a reservoir for BrO_x radicals and as an intermediate in a catalytic cycle that contributes to odd-oxygen destruction.[1−3] Laboratory investigations of bromine nitrate chemistry reported to date have focused on the kinetics of $BrONO_2$ formation via the $BrO + NO_2$ association reaction,[4−6] quantitative measurement of absorption cross sections[7−9] and photodissociation quantum yields,[2,10] and heterogeneous reactions of $BrONO_2$ that represent important nighttime sinks.[11,12] Because gas-phase reactions involving $BrONO_2$ have been thought to be unimportant as stratospheric $BrONO_2$ destruction pathways, they have received relatively little attention. A single measurement of the room-temperature rate coefficients for the reactions of ground-state bromine and chlorine atoms with $BrONO_2$ represents the entire literature database.[2]

$$Br(^2P_{3/2}) + BrONO_2 \rightarrow \text{products} \quad (1)$$

$$Cl(^2P_{3/2}) + BrONO_2 \rightarrow \text{products} \quad (2)$$

Harwood et al.[2] monitored the temporal profile of NO_3 appearance following 352.5 nm laser flash photolysis of $X_2/BrONO_2/N_2/O_2$ mixtures (X = Br, Cl), and used these data to obtain the 298 K rate coefficients $k_1 = (6.7 \pm 0.7) \times 10^{-11}$ cm^3 $molecule^{-1}$ s^{-1} and $k_2 = (1.27 \pm 0.16) \times 10^{-10}$ cm^3 $molecule^{-1}$ s^{-1}.

In this paper we report an experimental study of the kinetics of reactions 1−3 as functions of temperature (224−352 K) and pressure (16−250 Torr of N_2).

$$O(^3P_J) + BrONO_2 \rightarrow \text{products} \quad (3)$$

Kinetic information is obtained by monitoring the temporal profile of the reactant atom under pseudo-first-order conditions with $BrONO_2$ in large excess. The values for k_1(298 K) and k_2(298 K) obtained in this study agree well with their respective literature values, and we find that all three reactions are characterized by negative activation energies, i.e., the rate coefficients for all three reactions increase with decreasing temperature. Furthermore, we find that reaction 3 is fast enough to compete with photodissociation as a stratospheric $BrONO_2$ removal mechanism at altitudes above approximately 25 km.

Experimental Technique

The laser flash photolysis (LFP)−resonance fluorescence (RF) apparatus used in this study was similar to one we have employed in numerous previous studies of atom−molecule reactions involving Br,[13] Cl,[14] and O[15] atoms. A schematic diagram of the current version of the apparatus is published elsewhere.[10,16] Important features of the apparatus and experimental approach that are specific to this study are described below.

A Pyrex, jacketed reaction cell with an internal volume of ∼150 cm^3 was used in all experiments. The cell was maintained at a constant temperature by circulating ethylene glycol ($T >$ 298 K) or methanol ($T <$ 298 K) from a thermostated bath through the outer jacket. A copper−constantan thermocouple with a stainless steel jacket was periodically injected into the reaction zone through a vacuum seal to measure the gas temperature under the precise pressure and flow rate conditions of the experiment.

† Part of the special issue "Harold Johnston Festschrift".

* To whom correspondence should be addressed: School of Chemistry and Biochemistry, Georgia Institute of Technology, Atlanta, GA 30332-0400. E-mail: pw7@prism.gatech.edu.

‡ School of Earth and Atmospheric Sciences.

§ School of Chemistry and Biochemistry.

|| Present address: Department of Chemistry, Emory University, Atlanta, GA 30322.

10.1021/jp001947q CCC: $20.00
Published on Web 09/20/2000

Oxygen and chlorine atoms were produced by 355 nm laser flash photolysis of NO_2 and Cl_2, respectively, using third harmonic radiation from a Nd:YAG laser (Quanta Ray model DCR-2A) as the photolytic light source. In some experiments, oxygen atoms were generated by 248 nm laser flash photolysis of the $BrONO_2$ reactant using a KrF excimer laser (Lambda Physik model Compex 102) as the photolytic light source; it has been demonstrated that 248 nm photolysis of $BrONO_2$ produces O atoms with a relatively high yield of ~66%.[10,17] Bromine atoms were generated by laser flash photolysis of $BrONO_2$ at a variety of Nd:YAG and excimer laser wavelengths (248, 266, 308, and 355 nm); the sources of 248, 266, and 355 nm radiation were the lasers mentioned above, while the source of 308 nm radiation was a Lambda Physik model Lextra 200 excimer laser.

In experiments where Br kinetics were studied, approximately 0.5 Torr of CO_2 was added to the reaction mixture in order to rapidly deactivate any photolytically generated spin−orbit excited bromine atoms, $Br(^2P_{1/2})$; the rate coefficient for electronic-to-vibrational energy transfer from $Br(^2P_{1/2})$ to CO_2 is known to be 1.5×10^{-11} $cm^3 molecule^{-1} s^{-1}$.[18] Photodissociation of Cl_2 at 355 nm is known to produce >99% of the chlorine atoms in the $^2P_{3/2}$ ground state.[19,20] The three fine structure levels of $O(^3P_J)$ are sufficiently closely spaced in energy that it is safe to assume rapid equilibration via collisions with the N_2 buffer gas. The above considerations along with the magnitude of the observed rate coefficients (i.e., very fast) suggests that the reactant atoms in our studies of reactions 1−3 can be taken to be $Br(^2P_{3/2})$, $Cl(^2P_{3/2})$, and a thermalized mixture of $O(^3P_J)$ ($J = 0, 1, 2$), respectively.

An atomic resonance lamp, situated perpendicular to the photolysis laser, excited resonance fluorescence in the photolytically produced atoms. The resonance lamp consisted of an electrodeless microwave discharge through about one Torr of a flowing mixture containing a trace of Br_2, Cl_2, or O_2 in helium. Radiation passed from the lamp into the reaction cell through MgF_2 optics. The region between the lamp and the reaction cell was purged with a flowing gas filter mixture that effectively prevented simultaneous detection of multiple species.[13−15] For detection of Br, Cl, and O atoms, the filter gases were 50 Torr cm CH_4, 3 Torr cm N_2O, and 60 Torr cm O_2, respectively. Resonance fluorescence was collected by an MgF_2 lens on an axis orthogonal to both the photolysis laser beam and the resonance lamp beam, and imaged onto the photocathode of a solar blind photomultiplier. The region between the reaction cell and the photomultiplier was purged with N_2 to prevent absorption of resonance fluorescence by atmospheric gases such as O_2 and H_2O. Signals were processed using photon-counting techniques in conjunction with multichannel scaling.

To avoid accumulation of photolysis or reaction products, all experiments were carried out under "slow-flow" conditions. The linear flow rate through the reactor was typically 3.5 cm s^{-1} (range was 1.7−5.3 cm s^{-1}), and the laser repetition rate was typically 5 Hz (range was 2−10 Hz). Since photolysis occurred on an axis perpendicular to the direction of flow, no volume element of the reaction mixture was subjected to more than a few laser shots. The photolytic precursors NO_2 and Cl_2 were flowed into the reaction cell from 12 L bulbs containing dilute mixtures in nitrogen buffer gas, while CO_2 and additional N_2 were flowed directly from their high-pressure storage tanks. Bromine nitrate was introduced into the reaction cell by passing a flow of N_2 over the $BrONO_2$ sample that was kept in a trap at 220−230 K. The $BrONO_2$ flow was premixed with additional N_2 (and with CO_2 when appropriate) before entering the reaction cell. To prevent dark reactions of $BrONO_2$ with the photolytic precursors Cl_2 and NO_2, these species were injected into the reaction cell just upstream from the reaction zone. To minimize the rate of $BrONO_2$ hydrolysis on the walls of the flow system, N_2O_5 was flowed through the system for about 15 min before each series of experiments; this treatment converted nearly all adsorbed H_2O to gaseous HNO_3.

Species concentrations in the reaction mixtures were evaluated using a combination of photometric, mass−flow-rate, and total pressure measurements. The concentration of bromine nitrate was measured both upstream and downstream of the reaction cell by UV photometry. Both absorption cells were 200 cm in length, and cadmium penray lamps were used as the light source in both cells. Quantitative measurements of $BrONO_2$ were made in every experiment using 228.8 nm as the monitoring wavelength: the $BrONO_2$ absorption cross section at 228.8 nm was taken to be 2.17×10^{-18} cm^2.[7−9] Periodically, absorption measurements were also made at 326.1 nm (also a cadmium lamp emission line) in order to assess the level of Br_2O impurity in the $BrONO_2$ sample and the degree to which Br_2O was generated by hydrolysis of $BrONO_2$ on the walls of the slow flow system:

$$BrONO_2 + H_2O(\text{adsorbed}) \rightarrow HOBr + HNO_3 \qquad (4)$$

$$2\ HOBr \leftrightarrow Br_2O + H_2O \qquad (5)$$

The absorption cross section for $BrONO_2$ at 326.1 nm was taken to be 9.1×10^{-20} cm^2,[7−9] while absorption cross sections for Br_2O at 228.8 and 326.1 nm were taken to be 1.51×10^{-18} cm^2 and 2.04×10^{-18} cm^2, respectively.[21] Solution of two equations (one for total absorbance at 228.8 nm and one for total absorbance at 326.1 nm) in two unknowns yielded estimates of Br_2O impurity levels. To assess the possibility that some of the absorbance observed at 228.8 nm and/or at 326.1 nm resulted from material adsorbed to absorption cell windows, some additional experiments were carried out where a third (short) absorption cell with a path length of 10 cm was incorporated into the slow flow system. When the $BrONO_2/N_2$ mixture was flowing through the system, the 228.8 nm absorbances in the long and short absorption cells scaled as they should if all absorption was attributable to gas-phase species. However, the (much smaller) absorbances at 326.1 nm did not scale appropriately, i.e., the absorbance in the 10 cm cell was typically more than 5% of the absorbance in the 200 cm cell. Therefore, gas-phase absorbances at 326.1 nm were taken to be the difference between those observed in the long and short cells, and the path length used to convert absorbance to Br_2O concentration was taken to be 190 cm. To check impurity levels of Br_2 and NO_2 in $BrONO_2$ samples, some experiments were carried out where the flowing sample was passed through a multipass absorption cell that employed 457.9 nm radiation from an Ar^+ laser as the probe radiation and had a total absorption path length (88 passes) of ~3300 cm. Both Br_2 and NO_2 have absorption cross sections of 4.5×10^{-19} cm^2 at 457.9 nm.[22,23]

Bromine nitrate was synthesized from the reaction of BrCl with $ClONO_2$, as first described by Spencer and Rowland.[7] Chlorine nitrate ($ClONO_2$) was synthesized from the reaction of Cl_2O with N_2O_5 as first described by Schmeisser,[24] while Cl_2O was prepared by passing Cl_2(g) over solid yellow mercuric oxide as described by Cady[25] and N_2O_5 was prepared from the gas-phase reaction of NO_2 with O_3 as described by Ravishankara et al.[26] BrCl was prepared by mixing Br_2 with an excess of Cl_2 at 195 K as described by Burkholder et al.[8] Before being used

to prepare $BrONO_2$, the BrCl sample was purified by trap-to-trap distillation using a series of traps held at 195, 158, and 77 K. We found that it was easier to separate Br_2 from BrCl than it was to separate Br_2 from $BrONO_2$. Additional details concerning the syntheses of Cl_2O, N_2O_5, $ClONO_2$, BrCl, and $BrONO_2$ can be found elsewhere.[10]

The gases used in this study had the following stated minimum purities: N_2, 99.999%; CO_2, 99.99%; Cl_2, 99.99%; O_2, 99.99%; NO_2, 99.5%. The stated purities of Cl_2 and NO_2 refer to the liquid phase in the high-pressure storage cylinder. N_2, CO_2, and O_2 were used as supplied, while Cl_2 and NO_2 were degassed repeatedly at 77 K before being used to prepare dilute mixtures in N_2 buffer gas. Ozone was prepared by passing UHP O_2 through a commercial ozonator. It was collected and stored on silica gel at 195 K. The liquid Br_2 sample had a stated minimum purity of 99.94%; it was transferred into a vial fitted with a high vacuum stopcock and degassed repeatedly at 77 K before use.

Results and Discussion

1. Experimental Results. All experiments were carried out under pseudo-first-order conditions with $BrONO_2$ in large excess over the atomic reactant. Hence in the absence of secondary reactions that enhance or deplete the reactant atom concentration, the atom temporal profile is dominated by the reactions

$$A_i + BrONO_2 \rightarrow \text{products} \qquad i = 1-3 \qquad \text{(i)}$$

$$A_i + I_j \rightarrow \text{products} \qquad \text{(6j)}$$

$A_i \rightarrow$ loss by diffusion from the detector field of view and/or reaction with background impurities (7i)

In the above reaction scheme, A_i represents the reactant atom in reaction i, I_j is the jth impurity in the $BrONO_2$ sample, and "background" impurities are those which are present even when the $BrONO_2$ flow is shut off (including the photolytes Cl_2 and NO_2). Integration of the rate equations for the above scheme yields the relationship

$$\ln([A]_0/[A]_t) = \ln(S_0/S_t) = \{(k_i + \sum(\alpha_j k_{6j}))[BrONO_2] + k_{7i}\}t = k't \quad \text{(I)}$$

where S_0 and S_t represent the resonance fluorescence signal levels at times 0 and t, respectively, and α_j represents the ratio $[I_j]/[BrONO_2]$.

For all three reactions studied, atom temporal profiles were found to be exponential, and observed pseudo-first-order decay rates were found to increase linearly as a function of $BrONO_2$ concentration as predicted by eq I. Furthermore, observed temporal profiles were independent of laser fluence and varied as predicted by eq I when concentrations of the photolytic precursors NO_2 and Cl_2 were varied (if the atom reacts with its photolytic precursor at a significant rate, then k_{7i} will increase with increasing Cl_2 ($i = 2$) or NO_2 ($i = 3$) concentration even if the atom concentration is held constant as the photolyte concentration is varied). Typical atom temporal profiles are shown in Figure 1 and typical plots of k' versus $[BrONO_2]$ are shown in Figure 2. The kinetic data obtained for reactions 1−3 are summarized in Tables 1 − 3, and Arrhenius plots for reactions 1−3 are shown in Figure 3. For all three reactions, the Arrhenius plots are linear over the temperature range investigated, and all three reactions display small negative activation energies, suggesting that long-range attractive forces

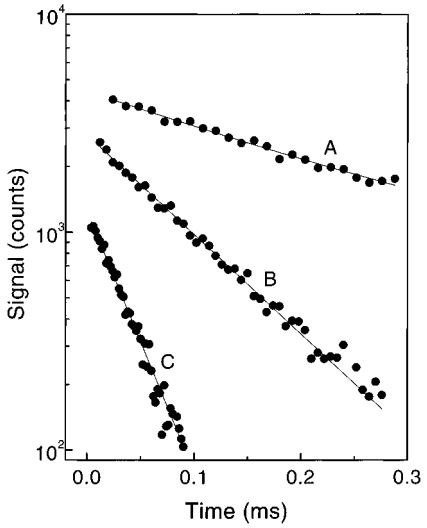

Figure 1. Typical resonance fluorescence temporal profiles observed in studies of reactions 1−3. Reaction: $O(^3P_J) + BrONO_2$. Experimental conditions: $T = 227$ K; $P = 50$ Torr; $[BrONO_2]$ in units of 10^{14} molecules cm^{-3} = (A) 0.80, (B) 2.04, (C) 5.16; number of laser shots averaged = (A) 2500, (B) 2600, (C) 3500. Solid lines are obtained from least squares analyses and give the following first-order decay rates in units of s^{-1}: (A) 3650, (B) 10500, (C) 25800.

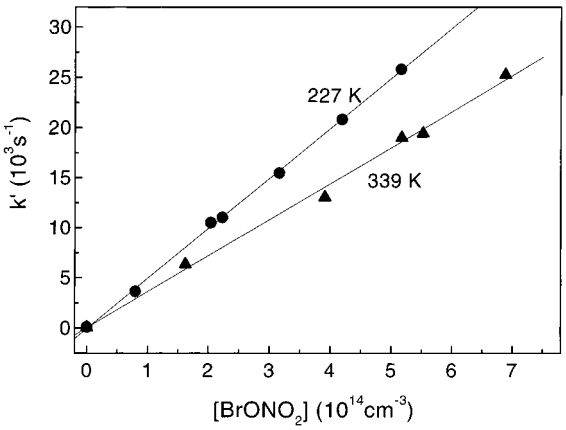

Figure 2. Typical plots of k' versus $[BrONO_2]$ for data obtained in studies of reactions 1−3. Reaction: $O(^3P_J) + BrONO_2$. Solid lines are obtained from least squares analyses; their slopes give the following bimolecular rate coefficients in units of 10^{-11} $cm^3 molecule^{-1} s^{-1}$: 4.99 at 227 K and 3.59 at 339 K.

play an important role in all three reactions. The following Arrhenius expressions are derived from the data:

$$k_1 = (1.78 \pm 0.33) \times 10^{-11} \exp\{(365 \pm 52)/T\} \text{ cm}^3 \text{ molecule}^{-1} \text{ s}^{-1}$$

$$k_2 = (6.28 \pm 1.28) \times 10^{-11} \exp\{(215 \pm 59)/T\} \text{ cm}^3 \text{ molecule}^{-1} \text{ s}^{-1}$$

$$k_3 = (1.91 \pm 0.34) \times 10^{-11} \exp\{(215 \pm 50)/T\} \text{ cm}^3 \text{ molecule}^{-1} \text{ s}^{-1}$$

Uncertainties in the above expressions are 2σ and represent precision only. The uncertainties in the above expressions refer to the Arrhenius parameters only. Realistic error estimates for individual rate coefficients are derived below. As described in eq I, the above Arrhenius expressions only represent the reactions of interest accurately if the rate of atom removal from

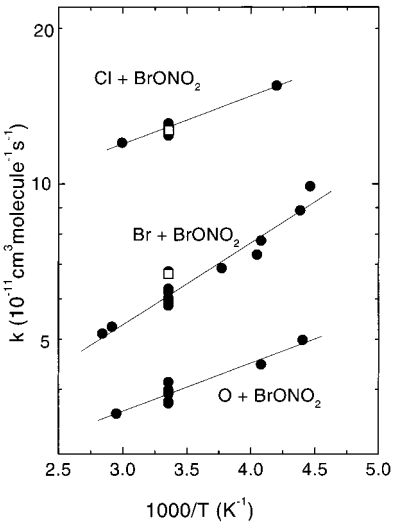

Figure 3. Arrhenius plots for reactions 1−3. The solid lines are obtained from least squares analyses (of data from this study only) and represent the Arrhenius expressions given in the text. Solid data points are from this study while open data points are from ref 2.

reactions with impurities that enter the reactor with the $BrONO_2$ flow (or are produced via dark reactions involving $BrONO_2$) is negligible compared to the rate of atom removal by $BrONO_2$ itself. Potential contributions from impurity reactions are assessed below.

2. Estimated Accuracy of Reported Rate Coefficients. Examination of Tables 1−3 shows that the precision of the rate coefficient measurements is quite good. However, systematic errors resulting from impurities in the $BrONO_2$ sample and from heterogeneous reactions in the slow flow system are potentially important and need to be addressed. In addition, the accuracy of $BrONO_2$ concentration measurements makes a significant contribution to the overall uncertainty in reported rate coefficients.

The absorption cross section for $BrONO_2$ at 228.8 nm is only known to about 10% accuracy,[8] and this source of uncertainty contributes directly to the uncertainties in our reported values for k_1-k_3. An additional source of uncertainty in our measured $BrONO_2$ concentrations results from the fact that, despite our best efforts to "condition" the flow system, some $BrONO_2$ was lost upon traversal of the system. In experiments with the reaction cell at 298 K and above, the $BrONO_2$ concentration measured downstream from the reaction cell was typically less than 5% lower than the concentration measured upstream from the reaction cell. However, at the lowest temperatures where kinetic data were obtained (∼225 K), the downstream $BrONO_2$ concentration was typically ∼30% lower than the upstream concentration. Apparently, more efficient binding of $BrONO_2$ to the reactor walls at lower temperatures facilitates heterogeneous reactions that destroy $BrONO_2$. All concentrations reported in Tables 1−3 are the averages of concentrations measured in the upstream and downstream absorption cells (corrected for small pressure gradients and, of course, for temperature differences between the absorption cells and the reaction cell). On the basis of the above considerations, we estimate the accuracy of measured $BrONO_2$ concentrations to be ±12% for kinetics experiments at $T \geq 298$ K, increasing to ±20% for kinetics experiments at $T \sim 225$ K.

As mentioned above, impurities that react rapidly with the atom reactants are sources of potential systematic error in measured rate coefficients *if* the impurity is present in the $BrONO_2$ sample or is produced by heterogeneous removal of $BrONO_2$ in the slow flow system. The impurities of this type that are most likely to contribute to $Br(^2P_{3/2})$, $Cl(^2P_{3/2})$, and/or $O(^3P_J)$ removal are Br_2, Br_2O, and NO_2; literature values and estimates (where data are unavailable) of the rate coefficients for these potential impurity reactions are summarized in Table 4.

As discussed in the Experimental Section, the sum of the impurity levels of Br_2 and NO_2 was evaluated using long path absorption at 457.9 nm as the probe technique. These observations showed that $([Br_2] + [NO_2])/[BrONO_2]$ was less than 0.03 in all bromine nitrate samples examined. Using the measurements of upper limit Br_2 and NO_2 levels in conjunction with the information in Table 4, we conclude that reactions of these impurities with the reactant atoms contributed ≤0.2% to the measured value of k_1, ≤3% to the measured value of k_2, and ≤1.5% to the measured value of k_3.

Despite our best efforts, the dual wavelength photometric measurements at 228.8 and 326.1 nm (see Experimental Section) could only constrain the Br_2O impurity level to be ≤10% of the $BrONO_2$ level. The relatively weak absorbance of Br_2O at 326.1 nm and some problems with weak absorption by material collected on absorption cell windows (see above) precluded more sensitive Br_2O measurements. Fortunately, additional information about the Br_2O-to-$BrONO_2$ concentration ratio in the reactor was attainable from studies of $BrONO_2$ photochemistry at 355 nm. The photochemistry results are (being) published elsewhere,[10,17] but the key findings relevant to establishing the Br_2O impurity level are summarized below: (1) The "apparent" bromine atom quantum yield $\Phi(Br)$ from $BrONO_2$ photodissociation at 355 nm is 0.77 ± 0.19 (error is 2σ); (2) The "apparent" ratio $\Phi(Br)/\Phi(BrO)$ from $BrONO_2$ photodissociation at 355 nm is 3.2 ± 1.0 (error is 2σ); (3) At 355 nm the Br_2O absorption cross section is a factor of 29 larger than the $BrONO_2$ absorption cross section;[7−9] and (4). On the basis of thermochemical considerations, the quantum yields for Br and BrO production from Br_2O photodissociation at 355 nm are equal, i.e., the channel producing 2Br+O is energetically forbidden. In the above discussion, an "apparent" quantum yield is one that includes contributions to the measured photoproduct from $BrONO_2$ photolysis and possibly from photolysis of impurities in the $BrONO_2$ sample as well. It is a virtual certainty that Br_2O is the only bromine-containing impurity which contributes significantly to generation of the observed photoproducts at $\lambda = 355$ nm (the contribution from Br_2 is very small). The maximum possible Br_2O level that could be present is the amount needed to generate all of the observed BrO; under the (almost certainly correct) assumption that the Br_2O photodissociation quantum yield is unity, this constraint places a very conservative upper limit value for $[Br_2O]/[BrONO_2]$ at 0.03. Assuming gas kinetic rate coefficients for all Br_2O impurity reactions (see Table 4) and a Br_2O impurity level of 3%, reaction with Br_2O would contribute 6−12% to the measured value for k_1, 4−5% to the measured value for k_2, and 12−17% to the measured value for k_3. In all cases, the maximum impurity contribution is at the highest temperature studied and the minimum contribution is at the lowest temperature studied. It is worth noting that a very low Br_2O impurity level could only be established in experiments involving 355 nm photolysis of reaction mixtures containing only the $BrONO_2$ sample and N_2 (i.e., no added reactant atom photolytic precursor). There is no reason to suspect higher Br_2O levels in other experiments and, in fact, values for k_1(298 K) measured using 355 nm photolysis of $BrONO_2$ as the $Br(^2P_{3/2})$ source are in good agreement with

TABLE 1: Summary of Kinetic Data for the Reaction $Br(^2P_{3/2}) + BrONO_2 \rightarrow$ Products

T^a	P^a	$\lambda^{a,b}$	$[BrONO_2]^a$	$[Br]_0^{a,c}$	no. of expts.[d]	range of k' [a]	$k^{a,e}$
224	52	266	1000−4090	8.0−24	4	6300−47800	9.89 ± 0.79
228	51	266	1050−3550	3.2−11	5	7310−30900	8.89 ± 0.83
245	52	266	1510−4480	4.9−20	10	12400−32500	7.77 ± 0.75
247	50	266	1440−3240	2.3−12	6	10700−23900	7.30 ± 0.34
265	50	266	1660−3930	1.9−12	5	11100−26800	6.87 ± 0.27
298	20	266	1420−3890	5.0−12	6	9780−26200	6.77 ± 0.22
298	24	248	1180−6470	0.5−3.4	5	4490−37400	5.83 ± 0.21
298	26	308	1480−7070	1.3−4.8	4	8520−40700	5.84 ± 0.21
298	48	266	1120−8520	2.1−11	19	6940−52300	6.23 ± 0.23
298	51	266	1580−4050	4.6−9.9	3	9370−24000	5.96 ± 0.22
298	51	355	1090−8670	3.0−23	17	5660−49900	5.82 ± 0.18
298	140	308	2170−5210	1.7−4.7	4	14000−32000	6.01 ± 0.39
298	201	355	880−7260	2.5−21	5	4150−42100	5.89 ± 0.15
298	206	266	1570−3220	5.8−12	4	9420−19700	6.19 ± 0.45
298	251	266	1020−4400	2.2−9.2	6	4850−27500	6.27 ± 0.19
343	51	266	1670−5770	3.6−18	5	8510−30800	5.29 ± 0.20
352	51	266	1270−3800	5.4−13	5	6530−19100	5.13 ± 0.20

[a] Units are T (K), P (Torr), λ (nm); concentrations (10^{11} per cm^3), k' (s^{-1}), k (10^{-11} cm^3 molecule^{-1} s^{-1}). [b] $\lambda \equiv$ photolysis laser wavelength. [c] Calculated based on the measured laser fluence and $BrONO_2$ concentration. [d] expt ≡ determination of a single pseudo-first-order decay rate. [e] Uncertainties are 2σ and represent precision only.

TABLE 2: Summary of Kinetic Data for the Reaction $Cl(^2P_{3/2}) + BrONO_2 \rightarrow$ Products[a]

T^b	P^b	$[BrONO_2]^b$	$[Cl_2]^b$	$[Cl]_0^{b,c}$	no. of expts.[d]	range of k' [b]	$k^{b,e}$
238	20	0−4530	320	12	5	23−68800	15.5 ± 0.8
298	21	0−4130	270	12	5	28−53900	13.1 ± 0.6
298	21	0−3520	170−280	6.8−16	11	32−43900	12.4 ± 0.6
298	100	0−3730	280	11	5	18−50400	13.1 ± 1.0
334	21	0−3500	210	8.9	5	51−40600	12.0 ± 0.8

[a] The photolysis laser wavelength was 355 nm in all experiments. [b] Units are T (K), P (Torr), concentrations (10^{11} per cm^3), k' (s^{-1}), k (10^{-11} cm^3 molecule^{-1} s^{-1}). [c] Calculated based on the measured laser fluence and Cl_2 concentration. [d] expt ≡ determination of a single pseudo-first-order decay rate. [e] Uncertainties are 2σ and represent precision only.

TABLE 3: Summary of Kinetic Data for the Reaction $O(^3P_J) + BrONO_2 \rightarrow$ Products

T^a	P^a	$\lambda^{a,b}$	$[BrONO_2]^a$	$[NO_2]^a$	$[O]_0^{a,c}$	no. of expts[d]	range of k' [a]	$k^{a,e}$
227	50	355	0−5160	140	6.8−8.6	6	87−25800	4.99 ± 0.12
245	50	355	0−5580	110	6.0−8.3	3	93−24700	4.47 ± 0.31
298	16	355	0−9450	95	6.7	5	156−37900	3.96 ± 0.11
298	21	248	930−4770	0	11−29	3	4510−19800	4.13 ± 0.07
298	33	248	0−8100	70−190	3.8−17	4	92−33300	3.99 ± 0.21
298	50	355	0−6010	95	5.7	5	141−24200	3.79 ± 0.39
298	100	248	910−2280	0	2.7−6.9	3	2470−8580	3.92 ± 0.96
298	157	355	0−11200	160	11	4	122−42300	3.76 ± 0.13
339	51	355	0−6880	90−140	5.5−7.7	5	78−25300	3.59 ± 0.24

[a] Units are T (K), P(Torr), λ (nm), concentrations (10^{11} per cm^3), k'(s^{-1}), k(10^{-11} cm^{3}molecule^{-1}s^{-1}). [b] $\lambda \equiv$ photolysis laser wavelength. [c] Calculated based on the measured laser fluence and photolytic precursor (NO_2 or $BrONO_2$) concentration. [d] expt ≡ determination of a single pseudo-first-order decay rate. [e] Uncertainties are 2σ and represent precision only.

values obtained using shorter wavelength photolysis to generate $Br(^2P_{3/2})$.

Considering the three most important factors that limit the accuracy of reported rate coefficients to be precision, determination of the $BrONO_2$ concentration, and contributions from impurity reactions, we estimate that the accuracy of reported rate coefficients falls in the range 15−25%. The room temperature determination of the fastest rate coefficient (k_2) is the most accurate, while the lowest temperature determination of the slowest rate coefficient (k_3) is the least accurate. The following format is widely used to express uncertainties in rate parameters that are used in modeling atmospheric chemistry:[27]

$$f(T) = f(298)\exp\{(\Delta E_a/R)(T^{-1} - 298^{-1})\} \qquad \text{(II)}$$

Applying eq II to our results leads to the following estimated

TABLE 4: Literature or Estimated Rate Coefficients for Potentially Important Impurity Reactions

reaction	k (298 K)[a]	E_a/R[a]	ref
$Br(^2P_{3/2}) + NO_2$	0.021 at 15 Torr	−814	39
	0.20 at 200 Torr	−788	39
$Br(^2P_{3/2}) + Br_2O$	20	0[b]	40
$Cl(^2P_{3/2}) + Br_2$	15	144	41
$Cl(^2P_{3/2}) + NO_2$	0.078 at 15 Torr	−765	42
	0.92 at 200 Torr	−740[c]	42
$Cl(^2P_{3/2}) + Br_2O$	20[d]	0[b]	
$O(^3P_J) + Br_2$	2.0	−40	41
$O(^3P_J) + NO_2$	1.06	−209	43
$O(^3P_J) + Br_2O$	20[d]	0[b]	

[a] Units of k(298 K) are 10^{-11} cm^3 molecule^{-1} s^{-1} and units of E_a/R are degrees Kelvin. [b] In the absence of data, it is assumed that $E_a/R = 0$. [c] In the absence of data, it is guesstimated that E_a/R is a little less negative at 200 Torr than at 15 Torr. [d] In the absence of data, it is assumed that k (298 K) is gas kinetic.

TABLE 5: Thermochemistry of X + $BrONO_2$ Reaction Channels (X = $Br(^2P_{3/2})$, $Cl(^2P_{3/2})$, $O(^2P_J)$)

reaction no.	reactants	products	$-\Delta_r H°$ (298 K)[a]
(1a)	$Br(^2P_{3/2}) + BrONO_2$	$\rightarrow Br_2 + NO_3$	49
(1b)		$\rightarrow Br_2 + NO + O_2$	33
(1c)		$\rightarrow Br_2O + NO_2$	7
(2a)	$Cl(^2P_{3/2}) + BrONO_2$	$\rightarrow BrCl + NO_3$	75
(2b)		$\rightarrow BrCl + NO + O_2$	58
(2c)		$\rightarrow ClNO_2 + BrO$	25
(3a)	$O(^3P_J) + BrONO_2$	$\rightarrow BrO + NO_3$	93
(3b)		$\rightarrow BrNO_2 + O_2$	220
(3c)		$\rightarrow BrONO + O_2$	187
(3d)		$\rightarrow BrOO + NO_2$	151
(3e)		$\rightarrow Br + NO_2 + O_2$	147
(3f)		$\rightarrow OBrO + NO_2$	106
(3g)		$\rightarrow BrO + NO + O_2$	76
(3h)		$\rightarrow BrNO + O_3$	67

[a] Units of $\Delta_r H°$ are kJ mol^{-1}.

parameters (subscripts are reaction numbers): $f_1(298) = 1.17$, $(\Delta E_a/R)_1 = 40$; $f_2(298) = 1.15$, $(\Delta E_a/R)_2 = 50$; $f_3(298) = 1.20$, $(\Delta E_a/R)_3 = 30$.

3. Comparison of Reported Rate Coefficients with Literature Values. As mentioned in the Introduction, the entire literature database concerning the kinetics of reactions 1−3 consists of a single 298 K measurement of k_1 and k_2 by Harwood et al.[2] These authors obtained their kinetic information from time-resolved observations of the reaction product NO_3. The results of Harwood et al.[2] are plotted along with our data in Figure 3. Clearly, the agreement between the two studies is excellent.

It is interesting to compare the kinetics of reactions 1−3 with available kinetic information for the analogous reactions with $ClONO_2$ replacing $BrONO_2$ as the molecular reactant:

$$Br(^2P_{3/2}) + ClONO_2 \rightarrow \text{products} \quad (8)$$

$$Cl(^2P_{3/2}) + ClONO_2 \rightarrow \text{products} \quad (9)$$

$$O(^3P_J) + ClONO_2 \rightarrow \text{products} \quad (10)$$

There are no kinetic data in the literature for reaction 8, but reactions 9 and 10 have been studied by several groups.[28−34] Like reaction 2, the $Cl(^2P_{3/2}) + ClONO_2$ reaction has a small negative activation energy; however, $k_2 \sim 13\ k_9$ at 298 K.[28−30] Unlike reaction 3, the $O(^3P_J) + ClONO_2$ reaction has a significant positive activation energy of ~3.5 kJ mol^{-1},[31,33,34] and $k_3 \sim 200\ k_{10}$ at 298 K. Theoretical studies that identify the structures and energetics of the transition states for reactions 1−3 and 8−10 would be very useful for developing a molecular level understanding of the kinetics and dynamics of these interesting reactions.

4. Reaction Mechanisms. Reactions 1−3 each have multiple sets of energetically accessible products as summarized in Table 5 (enthalpies of formation used to compute the enthalpies of reaction given in Table 5 are taken from DeMore et al.,[27] Chase,[35] and Orlando and Tyndall[36]). The experiments reported in this paper provide no information concerning the identity of the reaction products. However, through time-resolved studies of NO_3 production following laser flash photolysis of $X_2/BrONO_2/N_2/O_2$ mixtures, Harwood et al.[2] have obtained NO_3 yields of 0.88 ± 0.08 and 1.04 ± 0.24 for reactions 1 and 2, respectively. In a very recent study, Burkholder[37] has employed time-resolved detection of NO_3 following 248 nm laser flash photolysis of $O_3/BrONO_2/N_2$mixtures to show that the yield of NO_3 from reaction 3 is greater than 0.85. Hence, it appears that reactions of $Br(^2P_{3/2})$, $Cl(^2P_{3/2})$, and $O(^3P_J)$ with $BrONO_2$ proceed predominantly via channels 1a, 2a, and 3a, respectively. The reactions of $Cl(^2P_{3/2})$ and $O(^3P_J)$ with $ClONO_2$ are also known to produce NO_3 with near unit yield.[28,31]

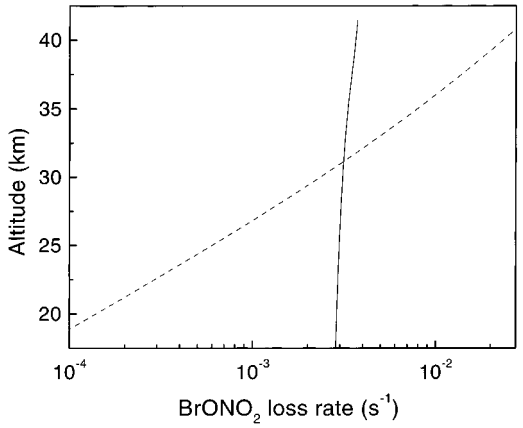

Figure 4. Altitude dependence of $BrONO_2$ destruction rates via photolysis (solid line) and reaction with $O(^3P_J)$ (dashed line) under conditions of 40° north latitude, March 15, local noon.

5. Implications for Atmospheric Chemistry. While kinetic information on all three of the reactions studied is useful for interpreting laboratory studies of $BrONO_2$ chemistry, it appears that only reaction 3 is an important stratospheric process. The rate coefficient for the $O(^3P_J) + BrONO_2$ reaction is high enough that this reaction can make a significant contribution to $BrONO_2$ removal in the stratosphere. Furthermore, since the dominant bromine-containing product of reaction 3 appears to be BrO,[37] the occurrence of reaction 3 affects stratospheric BrO_x levels. The value of k_3 reported in this study has been used in one modeling study which focused on polar lower stratospheric conditions and, as is appropriate for such conditions, incorporated heterogeneous as well as gas-phase chemistry of $BrONO_2$.[38] The inclusion of reaction 3, which has been ignored in all previous simulations of stratospheric bromine chemistry, increased stratospheric BrO levels by approximately 3%.[38] Because O atom concentrations increase dramatically with increasing altitude, the relative importance of reaction 3 (compared to photolysis) as a $BrONO_2$ destruction pathway, will increase with increasing altitude. First-order $BrONO_2$ removal rates via reaction 3 and via photolysis are plotted as a function of altitude in Figure 4. These altitude profiles, which are for 40° north latitude, March 15, local noon conditions, are constructed using the value for k_3 reported in this study in conjunction with the O atom altitude profile taken from ref 27 and $BrONO_2$ photolysis frequencies provided by R. W. Portmann of the National Oceanic and Atmospheric Administration's Aeronomy Laboratory. Reaction 3 becomes competitive with photolysis as a $BrONO_2$ loss process at altitudes above 25 km, and it becomes more important than photolysis at altitudes above 30 km. Although bromine nitrate chemistry is most important in the lower stratosphere, $BrONO_2$ is an important stratospheric Br_y species at altitudes up to 35 km[1]. It is clear that reaction 3 should be included in model simulations of stratospheric chemistry in order to correctly predict the partitioning of reactive bromine between its reservoir and catalytically active (i.e., Br and BrO) forms.

Acknowledgments. This research was supported by the National Aeronautics and Space Administration—Upper Atmosphere Research Program through Grants NAG5-3634 and

NAG5-8931. We thank R.W. Portmann for providing the altitude-dependent $BrONO_2$ photolysis rates and J.B. Burkholder for making his results on the products of the $O(^3P_J) + BrONO_2$ reaction known to us prior to publication.

References and Notes

(1) Lary, D. J. *J. Geophys. Res.* **1997**, *102*, 21515.
(2) Harwood: M. H.; Burkholder, J. B.; Ravishankara, A. R. *J. Phys. Chem. A* **1998**, *102*, 1309.
(3) Solomon, S. *Rev. Geophys.* **1999**, *37*, 275.
(4) Sander, S. P.; Ray G. W.; Watson, R. T. *J. Phys. Chem.* **1981**, *85*, 199.
(5) Danis, F.; Caralp, F.; Masanet, J.; Lesclaux, R. *Chem. Phys. Lett.* **1990**, *167*, 450.
(6) Thorn, R. P.; Daykin, E. P.; Wine, P. H. *Int. J. Chem. Kinet.* **1993**, *25*, 521.
(7) Spencer, J. E.; Rowland, F. S. *J. Phys. Chem.* **1978**, *82*, 7.
(8) Burkholder, J. B.; Ravishankara, A. R.; Solomon, S. *J. Geophys. Res.* **1995**, *100*, 16793.
(9) Deters, B.; Burrows, J. P.; Orphal, J. *J. Geophys. Res.* **1998**, *103*, 3563.
(10) Soller, R. Dissertation, Georgia Institute of Technology, Atlanta, 1998.
(11) Hanson, D. R.; Ravishankara, A. R. *Geophys. Res. Lett.* **1995**, *22*, 385.
(12) Hanson, D. R.; Ravishankara, A. R.; Lovejoy, E. R. *J. Geophys. Res.* **1996**, *101*, 9063.
(13) Jefferson, A.; Nicovich, J. M.; Wine, P. H. *J. Phys. Chem.* **1994**, *98*, 7128, and references therein.
(14) Piety, C. A.; Soller, R.; Nicovich, J. M.; McKee, M. L.; Wine, P. H. *Chem. Phys.* **1998**, *231*, 155 and references therein.
(15) Thorn, R. P.; Nicovich, J. M.; Cronkhite, J. M.; Wang, S.; Wine, P. H. *Int. J. Chem. Kinet.* **1995**, 369 and references therein.
(16) Finlayson-Pitts, B. J.; Pitts, J. N., Jr. *Chemistry of the Upper and Lower Atmosphere*; Academic Press: 2000; p 146.
(17) Soller, R.; Nicovich, J. M.; Wine, P. H. Manuscript in preparation.
(18) Peterson, A. B.; Wittig, C.; Leone, S. R. *Appl. Phys. Lett.* **1975**, *27*, 307.
(19) Busch, G. E.; Mahoney, R. T.; Morse, R. I.; Wilson, K. R. *J. Chem. Phys.* **1969**, *51*, 449.
(20) Park, J.; Lee, Y.; Flynn, G. W. *Chem. Phys. Lett.* **1991**, *186*, 449.
(21) Orlando, J. J.; Burkholder, J. B. *J. Phys. Chem.* **1995**, *99*, 1143.
(22) Hubinger, S.; Nee, J. B. *J. Photochem. Photobiol. A: Chem.* **1995**, *86*, 1.
(23) Schneider, W.; Moortgat, G. K.; Tyndall, G. S.; Burrows, J. P. *J. Photochem. Photobiol.* **1987**, *40*, 195.
(24) Schmeisser, M. *Inorg. Synth.* **1967**, *9*, 127.
(25) Cady, G. H. *Inorg. Synth.* **1957**, *5*, 156.
(26) Ravishankara, A. R.; Wine, P. H.; Smith, C. A.; Barbone, P. E.; Torabi, A. *J. Geophys. Res.* **1986**, *91*, 5355.
(27) DeMore, W. B.; Sander, S. P.; Golden, D. M.; Hampson, R. F.; Kurylo, M. J.; Howard, C. J.; Ravishankara, A. R.; Kolb, C. E.; Molina, M. J. Chemical Kinetics and Photochemical Data for Use in Stratospheric Modeling, Evaluation No. 12, Jet Propulsion Laboratory Publication 97−4; Jet Propulsion Laboratory: Houston, 1997.
(28) Yokelson, R. J.; Burkholder, J. B.; Goldfarb, L.; Fox, R. W.; Gilles, M. K.; Ravishankara, A. R. *J. Phys. Chem.* **1995**, *99*, 13976.
(29) Kurylo, M. J.; Knable, G. L.; Murphy, J. L. *Chem. Phys. Lett.* **1983**, *95*, 9.
(30) Margitan, J. J. *J. Phys. Chem.* **1983**, *87*, 674.
(31) Goldfarb, L.; Howard, M. H.; Burkholder, J. B.; Ravishankara, A. R. *J. Phys. Chem. A* **1998**, *102*, 8556.
(32) Adler-Golden, S. M.; Wiesenfeld, J. R. *Chem. Phys. Lett.* **1981**, *82*, 281.
(33) Kurylo, M. J. *Chem. Phys. Lett.* **1977**, *49*, 467.
(34) Molina, L. T.; Spencer, J. E.; Molina, M. J. *Chem. Phys. Lett.* **1977**, *45*, 158.
(35) Chase, M. W. *J. Phys. Chem. Ref. Data* **1996**, *25*, 1069.
(36) Orlando, J. J.; Tyndall, G. S. *J. Phys. Chem.* **1996**, *100*, 19398.
(37) Burkholder, J. B. *J. Phys. Chem. A* **2000**, *104*, 6733.
(38) Erle, F.; Grendel, A.; Perner, D.; Platt, U.; Pfeilsticker, K. *Geophys. Res. Lett.* **1998**, *25*, 4329.
(39) Kreutter, K. D.; Nicovich, J. M.; Wine, P. H. *J. Phys. Chem.* **1991**, *95*, 4020.
(40) Burkholder, J. B. *Int. J. Chem. Kinet.* **1998**, *30*, 571.
(41) Nicovich, J. M.; Wine, P. H. *Int. J. Chem. Kinet.* **1990**, *22*, 379.
(42) Ravishankara, A. R.; Smith, G. J.; Davis, D. D. *Int. J. Chem. Kinet.* **1988**, *20*, 811.
(43) Gierczak, T.; Burkholder, J. B.; Ravishankara, A. R. *J. Phys. Chem. A* **1999**, *103*, 877.